

Effect of Chain Tilt on the Interaction between Brush-Coated Colloids

M. W. Matsen

*Department of Physics, University of Reading, Whiteknights, Reading, RG6 6AF, U.K.**Received February 20, 2005; Revised Manuscript Received March 21, 2005*

ABSTRACT: The interaction between two spherical particles coated by end-grafted polymers immersed in a good solvent is examined using the strong-stretching theory of Milner, Witten, and Cates. Our calculation allows the polymer chains to tilt outward from the axis of closest approach, where the separation between the substrates is a minimum. This transfers the stress toward the extremity of the contact region, but to such a degree that the central chains can experience a reduction in free energy relative to the unperturbed brush. Nevertheless, the chain tilt has a small effect on the overall free energy, and thus the traditional Derjaguin approximation predicts a reasonably accurate interaction potential, provided the particles are large relative to the height of their brushes. Better yet, we propose an improved version that performs well for particles not much larger than the brushes.

I. Introduction

Many industrial applications rely on the uniform dispersion of colloidal particles in solution, but this can be difficult to achieve due to the notorious van der Waals attractions that generally cause the particles to aggregate. This has motivated considerable research into possible strategies for stabilizing suspensions against flocculation. One of the most effective remedies is the steric stabilization produced by end-grafting polymer chains to the surface of the particles (see Figure 1).¹ In a good solvent that swells the polymer brushes, the enthalpic penalty of overlapping brushes imparts a strong repulsion that adequately counters the van der Waals force. This repulsive interaction between swollen brushes also has relevance to solutions of block copolymer micelles and highly coordinated star polymers.²

Theoretical calculations^{2–5} for the interaction between polymeric brushes have historically been performed on flat parallel substrates, because of the substantial simplification that results from the translational symmetry. The true spherical geometry is then accounted for by applying the Derjaguin approximation,⁶ which requires the substrate separation to vary gradually as is the case for large particles. This approximation assumes that the chains only experience a simple compression normal to the substrate. For sufficiently small particles, however, the brush chains will squeeze out of the gap resulting in a significant lateral redistribution of segments, invalidating the Derjaguin approximation. Thus, at some point, it becomes necessary to perform the full calculation on the actual curved substrates.

In recent years, there have been several theoretical studies that explicitly include the spherical shape of the particles. Wijmans et al.⁷ performed the first using the lattice version of self-consistent field theory (SCFT),⁸ which was then followed by Roan^{9,10} using the continuum version of SCFT.¹¹ Cerdà et al.¹² have also investigated the interaction between brush-coated spheres using full three-dimensional Monte Carlo simulations. All of these calculations displayed severe departures from the Derjaguin approximation; that of Roan even predicted a weak attraction although this may be a consequence of numerical inaccuracy.¹³ In any

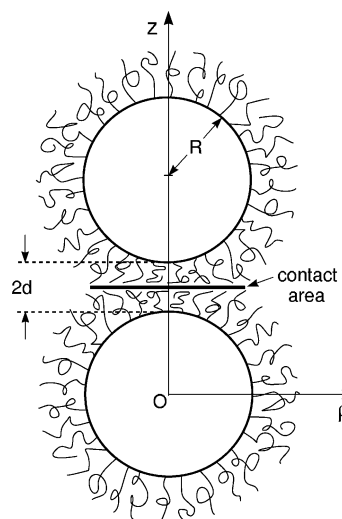


Figure 1. Two spherical particles of radius, R , coated by polymer brushes and separated by a distance, $2d$. The cylindrical coordinate system is positioned so that the z -axis passes through the particle centers at $z = 0$ and $z = 2(R + d)$. In the SST, there is a well-defined portion of each brush, the *contact region*, that presses against the opposing brush along a circular *contact area* in the $z = (R + d)$ plane.

case, the computational demands limited these studies to small spheres with diameters less than the brush thickness. In such extremes, there is no real surprise that the Derjaguin approximation breaks down. Here, we investigate the interaction over a range of larger particle sizes, to ascertain the point at which the Derjaguin approximation begins to fail. In the process of doing so, we also derive a much improved Derjaguin-like approximation.

II. Theory

Our calculation implements the strong-stretching theory (SST) of Milner, Witten, and Cates,¹⁴ which corresponds to the thick-brush limit of the continuum self-consistent field theory (SCFT).^{9,10,15} Both of these mean-field theories use a static field to represent the interactions experienced by a given polymer due to all the other molecules. The difference is that SST assumes the polymer chains are sufficiently stretched that their

configurations never deviate far from their ground-state trajectories. Under this assumption, the field simplifies to

$$w(\xi) = -\frac{3\pi^2\xi^2}{8a^2N} \quad (1)$$

where ξ is the distance from the grafting surface, N is the degree of polymerization of the brush chains, and a is the statistical segment length. The field must also be related self-consistently to the polymer concentration, $\phi(\xi)$, by

$$w(\xi) = v\phi(\xi) + \text{constant} \quad (2)$$

where v is referred to as the *excluded-volume* parameter. It accounts for the relative strength of the molecular interactions as well as the translational entropy of the background solvent, assuming that $\phi(\xi) \ll 1$. This condition is satisfied in the good-solvent regime, $v > 0$, where the polymer chains stretch outward from the grafting surface in order to maximize their contacts with the solvent.

Combining eqs 1 and 2, the brush profile can be expressed as

$$\phi(\xi) = \frac{3\pi^2}{8va^2N}(\alpha h_0^2 - \xi^2) \quad (3)$$

where h_0 is defined as the height of a fully extended brush and α is a parameter that increases from one as the brush is compressed. The height, h_0 , is determined by solving

$$\frac{\sigma NA}{\rho_0} = \int \phi(\xi) dV \quad (4)$$

with $\alpha = 1$ and no restriction on ξ . Here σ represents the grafting density, ρ_0^{-1} is the volume of a single segment, and A is the area of the grafting surface. If the brush is constrained to a height, $h < h_0$, then α must be increased appropriately so that eq 4 remains satisfied with the reduced height. Once the profile is determined, the free energy of the brush is given by

$$\frac{F}{k_B T} = \frac{3\pi^2\rho_0}{8a^2N^2} \int \xi^2 \phi(\xi) dV + \frac{v\rho_0}{2N} \int \phi^2(\xi) dV \quad (5)$$

where the first volume integral accounts for the entropy loss of the stretched chains and the second represents the molecular interactions.

For a flat brush (i.e., $dV = A d\xi$), the fully extended height is

$$\bar{h}_0 = \left(\frac{4\sigma v a^2 N^2}{\pi^2 \rho_0} \right)^{1/3} \quad (6)$$

and the corresponding free energy density is

$$\bar{f}_0 \equiv \frac{\bar{F}_0}{A} = \frac{9\pi^4 \rho_0 \bar{h}_0^5 k_B T}{160 v a^4 N^3} \quad (7)$$

From now on, we use these quantities of the uncompressed planar brush for our units of length and energy, which is done by setting $\bar{h}_0 = \bar{f}_0 \equiv 1$. When the flat brush is compressed to a height $\bar{h} < 1$,

$$\alpha = \frac{2}{3\bar{h}} + \frac{\bar{h}^2}{3} \quad (8)$$

and the free energy density becomes¹⁴

$$\bar{f} \equiv \frac{\bar{F}}{A} = \frac{5}{9\bar{h}} + \frac{5\bar{h}^2}{9} - \frac{\bar{h}^5}{9} \quad (9)$$

At this stage, the force between the two brush-coated spheres in Figure 1 can be estimated by the Derjaguin approximation.⁶ This assumes that the brush height changes gradually according to

$$\bar{h} = d + R - \sqrt{(R^2 - \rho^2)} \quad (10)$$

implying that the surface area over which the height lies between \bar{h} and $\bar{h} + d\bar{h}$ is given by $2\pi\rho d\rho = 2\pi(R + d - \bar{h}) d\bar{h}$. Thus, the excess free energy of the compressed brush on each particle is approximated by³

$$U(d) \approx 2\pi \int_d^1 (R + d - \bar{h})(\bar{f} - 1) d\bar{h} \quad (11)$$

$$\approx 2\pi R \int_d^1 (\bar{f} - 1) d\bar{h} \quad (12)$$

$$= 2\pi R \left(-\frac{5}{9} \ln(d) - (1 - d) + \frac{5}{27}(1 - d^3) - \frac{1}{54}(1 - d^6) \right) \quad (13)$$

from which the effective force is given by $-U'(d)$, where positive values correspond to a repulsive interaction. Note that the approximation made in eq 12 will prove to be irrelevant in comparison to the general inaccuracy of the Derjaguin approximation.

We now perform a more complete treatment, taking into account the curvature of the substrate and the tendency of the polymer chains to squeeze out of the gap between the two spheres. This is done by allowing the chains grafted to the sphere at a polar angle, θ , the freedom to tilt away from the surface normal by some angle, $\Psi(\theta)$. To evaluate the free energy for a specified tilt distribution, $\Psi(\theta)$, we adapt the approach by Olmsted and Milner,¹⁶ where the brush is split into a series of narrow wedges. To start, the particle surface is divided into a fine mesh, defined by the series of polar angles, $\theta_i = i\theta_M/M$, where $i = 0, 1, 2, \dots, M$. We use a sufficiently large number of mesh points, $M = 1000$, such that the discreteness becomes irrelevant. In practice, the mesh need not extend over the part of the sphere where the chain tilt is negligible; an upper limit of

$$\theta_M = \min \left\{ \pi, \frac{3}{R^{1/2}} \right\} \quad (14)$$

provides more than sufficient coverage. For each pair of mesh points, θ_{i-1} and θ_i , a wedge is constructed as illustrated in Figure 2. The wedge is defined by the coordinates of its vertex,

$$\rho_v = R \frac{\sin(\Psi_i) \sin(\theta_{i-1} + \Psi_{i-1}) - \sin(\Psi_{i-1}) \sin(\theta_i + \Psi_i)}{\sin(\theta_i - \theta_{i-1} + \Psi_i - \Psi_{i-1})} \quad (15)$$

$$z_v = R \frac{\sin(\Psi_i) \cos(\theta_{i-1} + \Psi_{i-1}) - \sin(\Psi_{i-1}) \cos(\theta_i + \Psi_i)}{\sin(\theta_i - \theta_{i-1} + \Psi_i - \Psi_{i-1})} \quad (16)$$

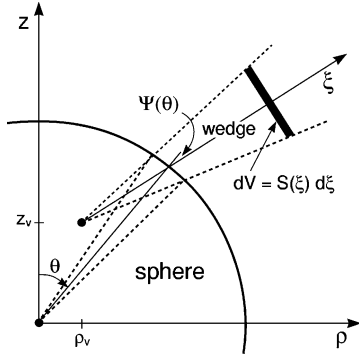


Figure 2. Construction of a wedge containing the polymer chains grafted to the spherical particle between the polar angles, $\theta \pm \Delta\theta/2$. The vertex of the wedge occurs at (ρ_v, z_v) with its two sides separated by an angle, $\Delta\theta + \Delta\Psi$, such that they tilt by angles, $\Psi \pm \Delta\Psi/2$, relative to the surface normal. An additional ξ axis is placed along the center of the wedge, which measures distances relative to the particle surface. The volume of the wedge is obtained by rotating its cross-section about the z axis, and the volume element, dV , is proportional to the total area, $S(\xi)$, normal to the ξ -axis contained within the wedge.

and the four angles,

$$\theta \equiv (\theta_{i-1} + \theta_i)/2 \quad (17)$$

$$\Delta\theta \equiv \theta_i - \theta_{i-1} \quad (18)$$

$$\Psi \equiv (\Psi_{i-1} + \Psi_i)/2 \quad (19)$$

$$\Delta\Psi \equiv \Psi_i - \Psi_{i-1} \quad (20)$$

where $\Psi_i \equiv \Psi(\theta_i)$. The number of chains contained within the wedge is given by αA , where

$$A = 2\pi R^2 \sin(\theta)\Delta\theta \quad (21)$$

The position of segments along the length of the wedge is specified relative to the particle surface with the coordinate, ξ . In terms of this coordinate, the vertex occurs at

$$\xi_v = \rho_v \sin(\theta + \Psi) + z_v \cos(\theta + \Psi) - R \cos(\Psi) \quad (22)$$

which is normally below the surface. In those cases where $\xi_v > 0$, the vertex always occurs well above the top of the brush. To perform volume integrals over the wedge, we also need the total area inside the wedge normal to the ξ -axis,

$$S(\xi) = 2\pi[\rho_v + (\xi - \xi_v) \sin(\theta + \Psi)](\xi - \xi_v)(\Delta\theta + \Delta\Psi) \quad (23)$$

which can be conveniently reexpressed in the quadratic form

$$S(\xi) = S_0 + S_1\xi + S_2\xi^2 \quad (24)$$

Using $dV = S(\xi) d\xi$ for the volume element, eq 4 implies a maximum brush extension, h_0 , given by

$$h_0^3 \left(S_0 + \frac{3}{8}S_1h_0 + \frac{1}{5}S_2h_0^2 \right) = A \quad (25)$$

However, the actual brush height will be

$$h = \min \left\{ h_0, \frac{R + d - R \cos(\theta)}{\cos(\theta + \Psi)} \right\} \quad (26)$$

because the chains cannot cross the $z = R + d$ midplane. To evaluate the segment profile in eq 3, we need

$$\alpha h_0^2 = \frac{2A + 3h^3 \left(\frac{1}{3}S_0 + \frac{1}{4}S_1h + \frac{1}{5}S_2h^2 \right)}{3h \left(S_0 + \frac{1}{2}S_1h + \frac{1}{3}S_2h^2 \right)} \quad (27)$$

which is derived from the conservation of segments, eq 4. Notice that outside the contact region where $h = h_0$, this expression gives $\alpha = 1$ as it should. Now that $\phi(\xi)$ has been determined, eq 5 provides the free energy density

$$f \equiv \frac{F}{A} = \frac{5h}{4A} \left(\alpha^2 h_0^4 \left(S_0 + \frac{1}{2}S_1h + \frac{1}{3}S_2h^2 \right) - h^4 \left(\frac{1}{5}S_0 + \frac{1}{6}S_1h + \frac{1}{7}S_2h^2 \right) \right) \quad (28)$$

To calculate the interaction potential, $U(d)$, we need to compare the free energy of the compressed brush to that of an isolated particle without tilted chains. For $\Psi(\theta) = 0$, the coefficients of $S(\xi)$ become $S_0 = A$, $S_1 = 2A/R$, and $S_2 = A/R^2$, which simplifies eq 25 to

$$h_0^3 \left(1 + \frac{3}{4} \frac{h_0}{R} + \frac{1}{5} \left(\frac{h_0}{R} \right)^2 \right) = 1 \quad (29)$$

Since the brush of an isolated particle is not compressed (i.e., $h = h_0$ and $\alpha = 1$), the free energy density in eq 28 reduces to

$$f_0 = h_0^5 \left(1 + \frac{5}{6} \frac{h_0}{R} + \frac{5}{21} \left(\frac{h_0}{R} \right)^2 \right) \quad (30)$$

Finally the interaction energy is evaluated by summing the excess free energy over all the wedges,

$$U(d) = \sum_{\text{wedges}} (f - f_0)A \quad (31)$$

The equilibrium tilt distribution, $\Psi_i \equiv \Psi(\theta_i)$, is obtained by minimizing the interaction energy, $U(d)$, subject to the boundary conditions, $\Psi_0 = \Psi_M = 0$. This is done by solving,

$$\frac{\partial}{\partial \Psi_i} U(d) = 0 \quad (32)$$

for $i = 1, 2, \dots, M - 1$. We use the Newton–Raphson method, which converges so rapidly that we gain one or two digits of accuracy every iteration. Because the required Jacobian

$$J_{ij} = \frac{\partial^2}{\partial \Psi_i \partial \Psi_j} U(d) \quad (33)$$

turns out to be a symmetric tridiagonal matrix, each iteration only takes a couple seconds (with $M = 1000$).

III. Results

We now begin by examining the equilibrium tilt distribution, $\Psi(\theta)$, plotted in Figure 3. (Since the edge of the contact area in Figure 1 occurs at $\theta^2 R \approx 2(1 - d)$ for large spheres, we scale the θ axis by $R^{1/2}$.) Just as expected, $\Psi(\theta)$ is strictly positive signifying that the chains all tilt away from the point of closest approach, where the gap between the spheres is narrowest.

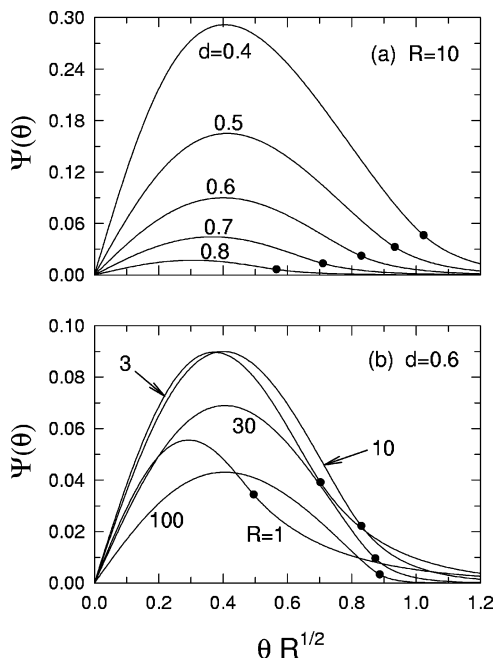


Figure 3. Tilt angle, $\Psi(\theta)$, of polymer chains grafted to the spherical particle at the polar angle, θ . Plot a shows a series of curves for spheres of radius, $R = 10$, at different separations, and plot b displays curves for spheres of different size at the fixed separation, $d = 0.6$. The solid dots denote the edge of the contact region. Note that our unit of length is the height, \bar{h}_0 , in eq 6 of an uncompressed flat brush.

Another general observation is that the tilt profile involves a relatively featureless peak located midway between the center of the contact region (i.e., $\theta = 0$) and its edge, denoted by the solid dots. Plot a demonstrates that the peak increases monotonically and gradually shifts toward larger θ as the two spheres approach each other. Plot b holds the separation constant and shows the effect of changing the sphere size; interestingly, the intermediate-sized spheres (i.e., $3 \lesssim R \lesssim 10$) show the greatest degree of chain tilt.

Figure 4 examines the free energy density, $f \equiv F/A$, as a function of the grafting location, θ . Again, plot a shows the effect of changing the separation, d , for a fixed particle size, R , while plot b shows the reverse. To illustrate the consequence of chain tilt, the dashed curves denote the distribution of free energy calculated without tilt (i.e., with $\Psi(\theta) = 0$), and the dotted curves give the Derjaguin approximation (i.e., eq 9 with $\bar{h} = d + \theta^2 R/2$). Notice that the zero-tilt and Derjaguin results are qualitatively similar; both predict a maximum energy density, f , at the center of the contact region that decreases monotonically to $f = f_0$ at the edge of the contact region, where the chains are no longer compressed. In any case, neither provide a good approximation for the equilibrium predictions (solid curves), other than when $R \gtrsim 100$. In general, the tilt produces a substantial redistribution of the free energy density with the chains at the center of the contact region benefiting from a massive energy reduction at the slight expense of those chains near the extremity of the contact region. By $R = 1$ [not shown in Figure 4b for reasons of clarity], the effect is so great that $f - f_0 < 0$ over the interval, $0 \leq \theta R^{1/2} \leq 0.360$, but this is compensated for by a positive peak centered at $\theta R^{1/2} = 0.483$, very near the edge of the contact region at $\theta R^{1/2} = 0.495$. Note that when the chains are permitted to tilt, $f - f_0$ remains significant for some distance beyond the contact region.

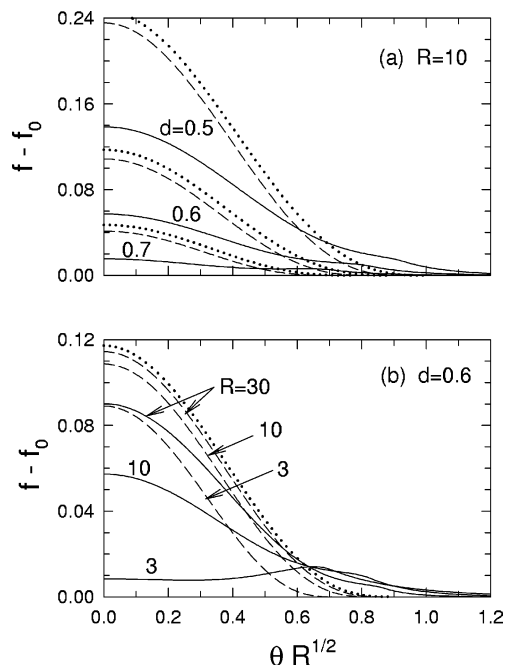


Figure 4. Free energy density, f , of chains grafted to the spherical particle at the polar angle, θ , relative to that, f_0 , of an isolated particle. Plot a shows a series of curves for spheres of radius, $R = 10$, at different separations, and plot b displays curves for spheres of different size at the fixed separation, $d = 0.6$. The dashed curves show equivalent results calculated without chain tilt (i.e., $\Psi(\theta) = 0$), and the dotted curves denote the traditional Derjaguin approximation. Note that our unit of free energy density is that, \bar{f}_0 , in eq 7 of an uncompressed flat brush.

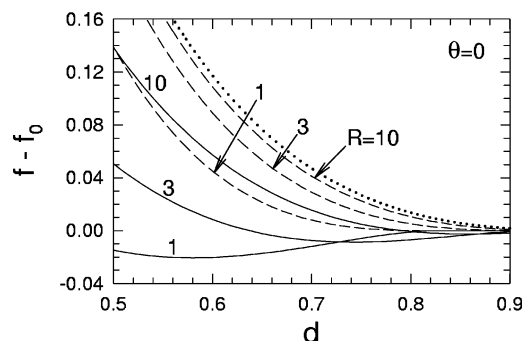


Figure 5. Analogous results to those in Figure 4, but concentrating just on the polymer chains at the center of the contact region (i.e., $\theta = 0$).

It is somewhat surprising that the greatest deviation from the Derjaguin approximation occurs at the point of closest approach, where the opposing substrates most resemble flat parallel planes. To illustrate the large discrepancy, the excess free energy density, $f - f_0$, at $\theta = 0$ is plotted in Figure 5 as a function of separation, d , for a range of particle sizes, R . Contrary to natural expectation, the free energy density, f , actually drops below the unperturbed value, f_0 , when the two brushes first come into contact, before it eventually increases monotonically. In contrast, the zero-tilt results (dashed curves) display a monotonic increase in f from the very first point of contact, which is reasonably well approximated by the Derjaguin approximation (dotted curve). This qualitative difference in behavior is most pronounced for small particles, where $f < f_0$ over a considerable interval of d . Of course, in the opposite limit of $R \rightarrow \infty$, the zero- and equilibrium-tilt results ultimately converge to the Derjaguin prediction.

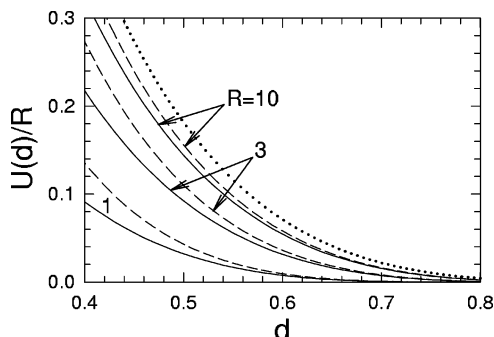


Figure 6. Interaction energy, $U(d)$, as a function of particle separation, d . The dashed curves show the zero-tilt approximation in eq 34 and the dotted curves denote the traditional Derjaguin approximation in eq 13.

Figure 6 plots the interaction energy, $U(d)$, obtained by integrating the free energy difference, $f - f_0$, over the surface area of the sphere. The solid curves plot $U(d)$ calculated with equilibrium tilt distributions, the dashed curves show equivalent results with zero tilt, and the dotted curve denotes the Derjaguin approximation from eq 13. Despite the occurrences of $f < f_0$ in Figure 5, we find that $U(d)$ strictly increases as the brushes are compressed, which implies a purely repulsive interaction. Although the three sets of curves in Figure 6 must all converge as $R \rightarrow \infty$, it is nevertheless surprising how accurate the zero-tilt results and the Derjaguin approximation are at finite R , given their poor performance in Figures 4 and 5. We attribute this to a fortuitous cancellation of errors; although the two approximations may seriously overestimate f at small θ , this is largely compensated for by their underestimation of f near the edge of the contact region.

IV. Discussion

The strong-stretching theory (SST) has become a standard method for modeling polymer brushes largely because of its convenient analytical form. Although our application to interacting spherical brushes requires some steps to be performed numerically, the computational demands are negligible in comparison to those of SCFT^{7,9,10} and Monte Carlo.¹² However, in using wedges to make our calculation tractable,¹⁶ it has been necessary to invoke a couple approximations beyond the basic assumption in SST that chain fluctuations about the ground-state trajectories are ignored. First of all, eq 5 overlooks the presence of zones where the free chain ends are excluded from next to convex grafting surfaces (i.e., wedges with $S'(\xi) > 0$).¹⁷ The proper treatment of these exclusion zones is sufficiently complex that the full solution has only been formulated for cylindrical brushes in the melt state (i.e., $\phi(\xi) = 1$).¹⁸ Nevertheless, this one example demonstrates that the zones have an absolutely negligible effect on the free energy, even in the limit of infinite surface curvature. Our more significant assumption is that the chain trajectories (i.e., wedges) remain straight. We cannot be certain how large the effect of chain curvature is, but it is presumably much smaller than that of the chain tilt (except perhaps when R and d are both very small). The one thing we can be certain of is that this extra degree of freedom will necessarily lower the free energy and thus reduce $U(d)$. Hence the Derjaguin approximation may be somewhat less accurate than indicated by our calculations.

Our prediction that chains near the center of the contact region (i.e., $\theta \approx 0$) experience a reduction in free energy when the brushes first come into contact was certainly unexpected. Nevertheless, it does coincide well with the SCFT calculations by Roan^{9,10} that predict $U(d)$ to become slightly negative, implying an attraction between small brush-coated particles. However, in our calculation, an actual reduction in the net free energy is impossible, which means $U(d) \geq 0$ for all d . The reason is simple; the equilibrium state of the brushes is obtained by minimizing the total free energy subject to the constraint that none of the chains cross the midplane, $z = R + d$. The reference state of two isolated particles is obtained by the same minimization but without the constraint, which means that its free energy, if anything, will be less. In fact, this argument can be extended to the SCFT calculations,¹³ which implies that the results of refs 9 and 10 are somehow tainted. Numerical inaccuracy resulting from the limited system size and mesh resolution permitted by the computationally demanding SCFT calculations is likely to blame.¹⁹

The nontilt (i.e., $\Psi(\theta) = 0$) curves for $U(d)$ in Figure 6 are considerably more accurate than that of the Derjaguin approximation. This leads us to propose the improved Derjaguin-like formula,

$$U(d) \approx 2\pi R^2(R + d) \int_d^{h_0} \frac{f - f_0}{(R + h)^2} dh \quad (34)$$

analogous to eq 11, but with the free energy density, f , evaluated for a uniformly compressed spherical brush rather than that of a flat brush. The upper limit, h_0 , and the reference energy density, f_0 , are provided by eqs 29 and 30, respectively. In this improved version, the integration variable, h , represents the distance to the contact area in the direction normal to the particle surface (i.e., eq 26 with $\Psi = 0$), whereas the \tilde{h} in eq 11 is the distance parallel to the z axis. This simple modification comes with no additional computational cost, since a uniformly compressed spherical brush is still a one-dimensional problem that can be easily evaluated by, for example, SCFT.²⁰ McConnell et al.⁴ implemented a similar improvement, although one that still uses eq 11. Unfortunately their description is confusing, and evidently their SCFT treatment of the spherical geometry evaluates the volume integrals incorrectly (see ref 15 for a correct implementation).

The improved eq 34 extends the range of the Derjaguin approximation to spheres as small as $R \sim 1$. The first reason for this marked improvement is that it accounts for the general chain relaxation resulting from the increased space available above a convex surface (i.e., $S'(\xi) > 0$). In particular, it incorporates the reduced brush height, h_0 , and free energy density, f_0 , of the unperturbed spherical brush, which are obviously crucial at the onset of the interaction where $d \approx h_0$. The second reason is that the redistribution of free energy resulting from the tilt has relatively little effect on the net free energy. This is because a positive tilt in Ψ_i reduces the energy of the i 'th wedge while at the same time increasing that of the $(i + 1)$ 'th wedge. Hence the reduction in free energy near $\theta \approx 0$ must be partially balanced by a rise in free energy elsewhere, specifically the extremity of the contact region. Naturally, we must remember that other quantities, such as the overall segment profile, will not benefit from such a fortunate

cancellation of errors, and thus the general validity of the zero-tilt assumption is still restricted to $R \gtrsim 100$.

The strong-stretching regime to which SST applies is undoubtedly beyond the reach of realistic experiments. Thus, our predictions for $U(d)$ are not expected to be quantitatively accurate, but presumably the qualitative features, including the unusual free energy distribution, will remain essentially the same for moderately stretched brushes. There is also no reason to expect our conclusions regarding the performance of the Derjaguin approximation to change much for the intermediate-stretched regime. Of course, it would be useful to confirm this with SCFT, but performing such calculations over a similar range of particle radii represents a major computational challenge. For now, we have to rely on the present SST predictions to gauge the validity of the Derjaguin approximations in eqs 11 and 34.

V. Conclusion

The interaction between two spherical particles coated by polymer brushes and immersed in good solvent (see Figure 1) has been investigated using the strong-stretching theory (SST) of Milner, Witten, and Cates¹⁴ combined with the wedge technique of Olmsted and Milner¹⁶ to control the chain orientation (see Figure 2). We find that, as the spherical brushes converge, the polymer chains tilt outward from the point of maximum compression transferring the chain stress toward the extremity of the contact region. This redistribution is so great that chains at the center of the contact region often experience a reduction in free energy relative to their unperturbed state. The effect of tilt only becomes negligible when the particle radius exceeds $R \gtrsim 100$ (measured relative to the thickness of a flat uncompressed brush). Nevertheless, the large reduction in free energy at the center of the contact region is partially balanced by a modest increase experienced by the many chains near the edge of the contact region, such that the effect of tilt on the net free energy is relatively small. As a consequence, the traditional Derjaguin approximation⁶ in eq 11, which neglects both the curvature of the particles and the resulting chain tilt, becomes accurate

at $R \gtrsim 10$, long before the tilt has vanished. This can also be improved upon by the Derjaguin-like approximation in eq 34, which accounts for the particle curvature and only neglects the chain tilt. This version, in fact, predicts a reasonable interaction potential, $U(d)$, for particles not much larger than the thickness of their brushes.

Acknowledgment. This work was supported by the EPSRC (GR/N36721).

References and Notes

- (1) Napper, D. H. *Polymeric Stabilization of Colloidal Dispersions*; Academic Press: New York, 1983.
- (2) Gast, A. P. *Langmuir* **1996**, *12*, 4060.
- (3) Mewis, J.; Frith, W. J.; Strivens, T. A.; Russel, W. B. *AIChE J.* **1989**, *35*, 415. Genz, U.; D'Aguzzo, B.; Mewis, J.; Klein, R. *Langmuir* **1994**, *10*, 2206.
- (4) McConnell, G. A.; Lin, E. K.; Gast, A. P.; Huang, J. S.; Lin, M. Y.; Smith, S. D. *Faraday Discuss. Chem. Soc.* **1994**, *98*, 121. Lin, E. K.; Gast, A. P. *Macromolecules* **1996**, *29*, 390.
- (5) Borukhov, I.; Leibler, L. *Macromolecules* **2002**, *35*, 5171.
- (6) Derjaguin, B. V. *Kolloid Z.* **1937**, *69*, 155.
- (7) Wijmans, C. M.; Leermakers, F. A. M.; Fleer, G. J. *Langmuir* **1994**, *10*, 4514.
- (8) Scheutjens, J. M. H. M.; Fleer, G. J. *J. Phys. Chem.* **1979**, *83*, 1619.
- (9) Roan, J. R. *Phys. Rev. Lett.* **2001**, *86*, 1027. Roan, J. R. *Phys. Rev. Lett.* **2001**, *87*, 059902.
- (10) Roan, J. R.; Kawakatsu, T. *J. Chem. Phys.* **2002**, *116*, 7295.
- (11) Edwards, S. F. *Proc. Phys. Soc. (London)* **1965**, *85*, 613.
- (12) Cerdà, J. J.; Sintes, T.; Toral, R. *Macromolecules* **2003**, *36*, 1407.
- (13) Matsen, M. W. *Phys. Rev. Lett.* Submitted for publication.
- (14) Milner, S. T.; Witten, T. A.; Cates, M. E. *Macromolecules* **1988**, *21*, 2610.
- (15) Dan, N.; Tirrell, M. *Macromolecules* **1992**, *25*, 2891.
- (16) Olmsted, P. D.; Milner, S. T. *Phys. Rev. Lett.* **1994**, *72*, 936. Olmsted, P. D.; Milner, S. T. *Phys. Rev. Lett.* **1995**, *74*, 829.
- (17) Wijmans, C. M.; Zhulina, E. B. *Macromolecules* **1993**, *26*, 7214. Li, H.; Witten, T. A. *Macromolecules* **1994**, *27*, 449.
- (18) Ball, R. C.; Marko, J. F.; Milner, S. T.; Witten, T. A. *Macromolecules* **1991**, *24*, 693.
- (19) Roan, J. R. Private communication.
- (20) The SCFT for a uniformly compressed spherical brush is identical to that of the isolated one treated in ref 15, except that a reflecting boundary is placed at a radius, $r = R + h$.

MA050362X